Available online at www.sciencedirect.com
SCIENCE DIRECT®
Journal of Solid State Chemistry 178 (2005) 3729–3734
JOURNAL OF SOLID STATE CHEMISTRY
www.elsevier.com/locate/jssc

Syntheses and characterization of the samarium(III)–copper(II) 3D coordination network constructed by iminodiacetic acid

Yue-Peng Cai[a,*], Guo-Bi Li[a], Qing-Guang Zhan[a], Feng Sun[a], Jiang-Gao Zhang[b], Song Gao[a], An-Wu Xu[c,**]

[a]*Department of Chemistry, South China Normal University, Guangzhou 510631, PR China*
[b]*School of Physics and Telecommunication Engineering, South China Normal University, Guangzhou 510631, PR China*
[c]*School of Chemistry and Chemical Engineering, Sun Yet-sen University, Guangzhou 510275, PR China*

Received 7 July 2005; received in revised form 18 September 2005; accepted 20 September 2005
Available online 26 October 2005

Abstract

The hydrothermal reaction of Sm_2O_3 with iminodiacetic acid (H_2Idad), CuO, and H_2O with a mole ratio of 1:2:4:300 resulted in the formation of one nanoporous 3D open framework Cu(II)–Sm(III) coordination polymer, $[\{Sm_2Cu_3(Idad)_6\}\cdot 8H_2O]_n$. Investigation shows that the coordination polymer possesses high thermal and structural stability. Temperature-dependent magnetic susceptibilities of the coordination polymer with the similar structure, $[\{Gd_2Cu_3(Idad)_6\}\cdot 8H_2O]_n$, were studied.

Keywords: Lanthanide(III)–copper(II) coordination polymers; Iminodiacetic acid; Crystal structures; Temperature-dependent magnetic susceptibilities; The thermal stabilities

1. Introduction

Over the past several decades, a variety of zeolites and open framework inorganic solids containing nanosized pores or channels with controlled sizes, shapes, and chemical environments have been developed, which has drawn much attention because they have potential applications in pharmaceutical manufacture, separation, catalysis, molecular recognition, and optoelectronic application [1]. In recent years, studies on coordination polymers as organic zeolite-like solids, built up from metals and multifunctional organic ligands, represent a rapidly expanding field. The "modular" approach has been successfully employed in the construction of metal-organic open-framework materials and various tailored organic building blocks and metal ions have been used to assemble a variety of nanoporous three-dimensional networks [2]. Although these efforts have contributed greatly to our understanding of how to build such solid-state structures, we still need to explore new building blocks and building principles before we are truly able to design and build versatile architectures with specific functions such as superconducting and magnetic properties [3].

On the other hand, lanthanide–transition metal complexes are good models for investigating the nature of the magnetic exchange interactions between 3*d* and 4*f* metal ions in magnetic materials that contain rare earth metals [4]. Since the high coordination number of *Ln*(III) may render structural flexibility and increase the thermodynamic stability, this aspect has attracted considerable attention and a great number of structural types of lanthanide–transition metal complexes have been reported [5]. However, many such studies have focused on discrete or infinite chain complexes, which were synthesized from conventional self-assembly reaction in solution or hydrothermal synthetic method, studies on lanthanide–transition metal organic complexes with nanoscale porous three-dimensional open-framework are still poorly explored [6,7].

*Corresponding author. Fax: +86 20 85210763.
**Also to be corresponded.
E-mail address: ypcai8@yahoo.com (Y.-P. Cai).

0022-4596/$ - see front matter © 2005 Elsevier Inc. All rights reserved.
doi:10.1016/j.jssc.2005.09.033

Our previous investigation of metal complexes with the branched unsymmetrical tripodal ligand *N*-[*N*′-(carboxymethyl)benzimidazol-2-yl-methyl]-*N*,*N*-bis(benzimidazol-2-ylmethyl)amine (HACntb) or symmetrical tris(2-benzimidazolylmethyl)amine (ntb)/tris(1-benzimidazolylmethyl)amine (nteb) has revealed that C_3-symmetric ntb can encapsulate lanthanide(III) ions to afford large hexafunctional hydrogen-donor building blocks, which were further assembled to form doubly interpenetrating three-dimensional steroisomeric networks with large cavities [8]. However, more flexible ligand nteb was employed to obtain two interesting complexes [9]. One is chiral due to the same clockwise ($\Delta\Delta$) or anticlockwise ($\Lambda\Lambda$) arrangements of two tripodal ligands, but two opposite enantiomers co-crystallize to form a racemate. While the other can be described as a mesocate ($\Delta\Lambda$) because two tripodal ligands in the same molecule present clockwise and anticlockwise conformation, respectively. And unsymmetric HACntb may chelate copper(II) ions to assembly an open, three-dimensional network of nanoscale porosity by N–H···O hydrogen bonds [10]. These findings prompted us to utilize tailored secondary building units (SBUs) to fabricate nanoporous *Ln*–Cu supramolecular network with magnetic properties. To achieve this goal, iminodiacetic acid (H_2Idad) was employed as initial reagents by hydrothermal synthesis, and one complex $[\{Sm_2Cu_3(Idad)_6\}\cdot 8H_2O]_n$ with three-dimensional (3D) network of nanoscale porosity was isolated and characterized.

2. Experimental

2.1. Materials and measurements

All materials were reagent grade obtained from commercial sources and used without further purification. Elemental analyses were performed on a Perkin-Elmer 240C analytical instrument. IR spectra were recorded on a Nicolet FT-IR-170SX spectrophotometer in KBr pellets. The magnetic susceptibility data was collected from polycrystalline samples at an external field of 1 T on a MPMS XL-7 magnetometer (Quantum Design) in the temperature range 2–300 K. The output data were corrected for the diamagnetism of the sample holder and the samples calculated from their Pascal's constants. Thermal gravimetric analysis was performed on a Shimadzu TGA-50H instrument.

2.2. Preparation of coordination polymers

$[\{Sm_2Cu_3(Idad)_6\}\cdot 8H_2O]_n$(1). A mixture of Sm_2O_3 (0.087 g, 0.25 mmol), CuO (0.040 g, 0.5 mmol), iminodiacetic acid (0.133 g, 1.0 mmol), and H_2O (20 ml) in a mole ratio of about 1:2:4:300 was heated in a 25-ml stainless-steel reactor with a Teflon liner at 140 °C for 80 h, blue crystals of **1** were isolated in about 78% yield (1.665 g) (based on Cu). Elemental analysis calcd. for $C_{24}H_{46}N_6O_{32}Cu_3Sm_2$ (%): C 20.25, H 3.23, N 5.91; found: C 20.21, H 3.29, N 5.94.

$[\{Gd_2Cu_3(Idad)_6\}\cdot 8H_2O]n$(2). The reaction procedure was the same as that of the compound $[\{Sm_2Cu_3(Idad)_6\}\cdot 8H_2O]_n$ except that Gd_2O_3 was used instead of Sm_2O_3. The pale blue crystals of **2** were isolated in about 69% yield (1.487 g) (based on Cu). Elemental analysis calcd. for $C_{24}H_{46}N_6O_{32}Cu_3Gd_2$ (%): C 20.00, H 3.00, N 5.00; found: C 20.08, H 2.95, N 4.94.

2.3. Crystallography

A suitable deep blue single crystal was mounted on a glass fiber and the intensity data were collected on a Bruker SMART CCD diffractometer with graphite monochromated Mo$K\alpha$ radiation ($\lambda = 0.71073$ Å) at 293 K. Absorption corrections were performed using the SADABS program [11]. The structure was solved by direct methods and refined by full-matrix least-squares against F^2 of data using SHELXTL software [12]. Anisotropic displacement parameters were assigned to all of the non-hydrogen atoms while the hydrogen atoms were included in the calculations isotropically but not refined. A summary of parameters for the data collections and refinements are given in Table 1. Supplementary crystallographic data were deposited at the Cambridge Crystallographic Data Center (CCDC) No. 255000.

3. Results and discussion

3.1. Thermogravimetric analyses of complex 1

The TGA curve for a crystalline sample of the compound **1** shows two weight-loss steps accompanied by

Table 1
Crystal data and structure refinement for complex $[\{Sm_2Cu_3(Idad)_6\}\cdot 8H_2O]_n$

Empirical formula	$C_{24}H_{46}N_6O_{32}Cu_3Sm_2$
Formula weight (g/mol)	1421.99
Crystal color	Green
Crystal system	Trigonal
Space group	$P\bar{3}c1$
Wavelength (Å)	0.71073
a (Å)	13.377(1)
b (Å)	13.377(1)
c (Å)	14.462(2)
γ (°)	120.00
V (Å^3)	2241.2(4)
Z	2
F(000)	1398
Temperature (K)	301(2)
μ (mm^{-1})	4.087
θ range (°)	1.76–27.53
R(int)	0.0378
No. refined parameters	113
No. reflections [$I>2\sigma(I)$]	1185
$R1$ [$I>2\sigma(I)$]	0.0274
w$R2$ [$I>2\sigma(I)$]	0.0784
Goodness of fit: S	1.091
Largest diff. peak and hole (e nm^{-3})	891/−957

two endothermic peaks. The first of 11.543% between 22.7 and 120.5 °C corresponds to the loss of eight solvated water molecules (calculated: 10.14%). The major weight loss (44.181%) occurred in the range 308–500 °C, which may correspond to complete destruction of the network. Single crystals of the compound were dehydrated but readily reabsorb water to regenerate a variant of the original structure that contains slightly less water in a few hours under atmospheric conditions, as confirmed by EA and TGA. This study indicated that the guest water molecules could not only escape from the channels, but could also be included into channels even at room temperature. Hence the totally dehydrated form must retain the same framework topology, and we are currently investigating its ability to absorb small molecules.

3.2. Structure description of complex 1

Crystallographic analysis revealed that, connected by bridging $Idad^{2-}$ ligands, the compound forms a nanoporous three-dimensional open framework based on a Sm_2Cu_3 secondary building unit (SBU), in which two Sm1 atoms are located on a threefold axis occupying two apical positions, while the three Cu1 ions lie in the basal trigonal plane, and the Sm1…Cu1, Sm1a…Cu1a separations are 6.166(4) and 4.559(3) Å, respectively; thus the Sm_2Cu_3 unit is very similar to an elongated trigonal bipyramid (see Fig. 1).

Additionally, each Sm ion is nine-coordinated, surrounded by nine carboxylic oxygen atoms from six neighboring $Idad^{2-}$ ligands (average Sm–O 2.481(4) Å), with the six carboxylate oxygen atoms, O1, O1a, O1b and O4, O4a, O4b forming a trigonal prism, while the other three carboxylate oxygen atoms as capping atoms (Fig. 2(a)). The copper ion is six coordinated to four carboxylate oxygen atoms and two nitrogen atoms of two ligands (with Cu–O bond lengths of Cu1–O1 2.411(5), Cu1–O3 1.954(3) Å and Cu–N bond length of Cu1–N1 2.015(4) Å. The bonding angles of O1–Cu1–O3 and O1–Cu1–N1 are 89.3(2), 90.7(1) and 73.3(1), 106.7(1)°, respectively). The geometry of the Cu^{2+} ion can best be described as distorted octahedron with the two axial bonds elongated, resulting from the Jahn-Teller effect (Fig. 2(b)) (see Table 2).

The six apical to base edges of each trigonal bipyramid Sm_2Cu_3 unit are composed of three long sides of Sm_1–O_4–C_3–O_3–Cu_1 with a mean Sm–Cu separation of 6.166(6) Å and three short sides of Sm_1–O_1–Cu_1 with a Sm–Cu separation of 4.559(3) Å. Such Sm_2Cu_3 core is connected by ligands $Idad^{2-}$ to give a C_3 symmetrical $[Sm_2Cu_3(Idad)_6]$ cluster as building blocks. Around each core Sm_2Cu_3, there are six other SBUs linked reversely along its six edges, forming a four metal rectangle framework sharing the edges with the two trigonal bipyramidal cores Sm_2Cu_3 (Fig. 1). In other words, each Sm_2Cu_3 core is connected with six other SBUs through six rectangle frameworks. These are then further extended to

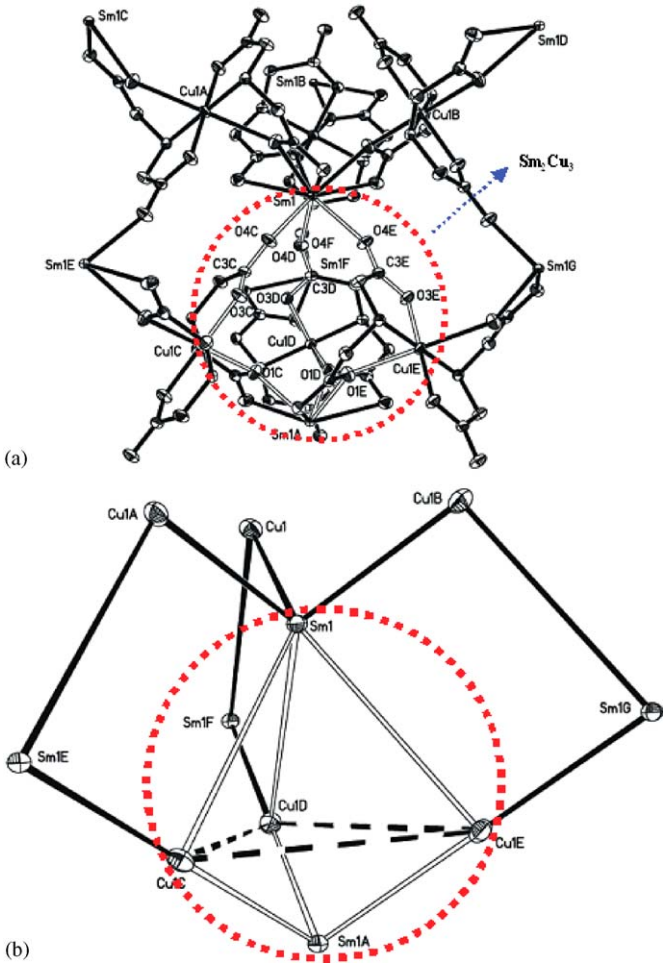

Fig. 1. (a) ORTEP view containing a secondary building unit (SBU) in $[\{Sm_2Cu_3(Idad)_6\}\cdot 8H_2O]_n$. Atoms labeled A, B, C, D and E are symmetry generated. (b) Trigonal bipyramid geometry of SUB base on metal ions bridged by carboxylate anions (thermal ellipsoids are shown at 30% probability).

form an open framework with an intersecting three-dimensional parallel-pipe hexagonal 12 metal channels extending along the crystallographic *c*-axis (Fig. 3), which houses water molecules and some of which are hydrogen bonded with oxygen atoms of the framework (the relative hydrogen bond distances and angles in Table 3). Each channel is surrounded by six other channels, so these hexagons can be arranged in close-packed honeycomb grids. The approximate diameters of the narrowest cross section of the 12 metal ring is 9.48 Å. Allowing for the van der Waals' radii of the atoms leaves approximately 7.5 Å of free space between opposite vertices and the free pore volume of the structure is 10.2%, based on the calculation approach adopted by Yaghi et al. [13] (Fig. 3). When the bound water molecules are removed, the volume increases up to 27.8%, which implies that the formation of microporous materials with lanthanide–copper organic, ordered, pore channels or/and microporous crystalline walls similar to the structure of the compound is possible. The wall of the hexagonal 12 metal channels includes

four metal windows (Figs. 1 and 3), resulting in an unprecedented 3D intersecting-channel lanthanide–copper organic framework.

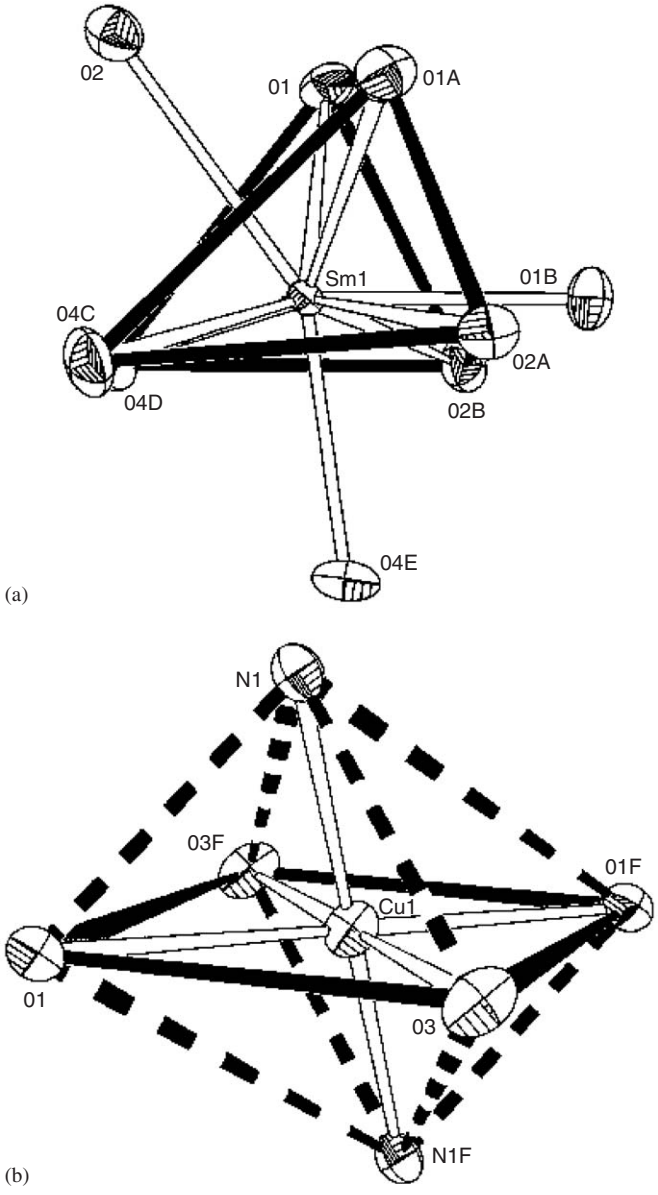

Fig. 2. Coordination geometry of the metal centers in $[\{Sm_2Cu_3(Idad)_6\}\cdot 8H_2O]_n$ (thermal ellipsoids are shown at 60% probability).

By the above analyses, we may understand that the hexagonal channel of this compound is actually enclosed by the six infinite alternately reverse C_3 symmetic columns, formed by connection of SBUs head-to-tail along the axial direction. These columns eventually turns into the hexagonal open-framework structure (Fig. 3). This structure not only demonstrates that the shape and symmetry of a SBU can induce a specific crystal structure, but also provides a new strategy to fabricate open framework with linear hexagonal channels by flexible organic ligand. This structure may provide further insight into designing new porous materials as well as other supramolecular architectures containing lanthanide–transition metals.

3.3. Magnetism of complex 2

In a series of analogous *Ln*(III)–Cu(II) compounds, Gd(III) has a $^8S_{7/2}$ free-ion ground state, without first-order angular momentum. The magnetic properties allow us to determine the nature and the magnitude of the Gd(III)–Cu(II) interaction. Though the structures of *Ln*(III)–Cu(II) (*Ln* = Gd, Nd, Eu, La) compounds bridged via diglycolic acid $O(CH_2COO)_2^{2-}$ and $Idad^{2-}$ ligand was reported by Ren et al. [7b] and Mao et al. [14] their

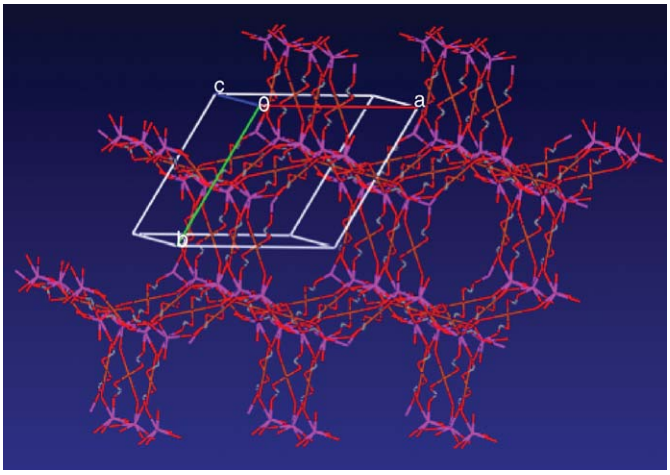

Fig. 3. Projection of the 3D framework down the *c*-axis in $[\{Sm_2Cu_3(Idad)_6\}\cdot 8H_2O]_n$, exhibiting large 12 metal membered hexagonal channels. The hydrogen atoms and water guests are omitted for clarity.

Table 2
Selected bond lengths (Å) and bond angles (°) of complex $[\{Sm_2Cu_3(Idad)_6\}\cdot 8H_2O]_n$

Bond distances		Bond angles			
Cu(1)–O(1)	2.411(3)	N(1)–Cu(1)–O(1)	73.18(14)	O(1)–Sm(1)–O(2B)	68.59(12)
Cu(1)–O(3)	1.954(3)	N(1)–Cu(1)–O(1F)	106.82(14)	O(2B)–Sm(1)–O(4D)	79.56(12)
Cu(1)–N(1)	2.015(4)	N(1)–Cu(1)–O(3)	94.43(15)	O(1)–Sm(1)–O(1A)	80.96(13)
Sm(1)–O(1)	2.388(3)	N(1)–Cu(1)–O(3F)	85.57(15)	O(2A)–Sm(1)–O(2B)	115.43(5)
Sm(1)–O(2)	2.707(4)	O(1)–Cu(1)–O(3)	90.67(14)	O(4C)–Sm(1)–O(4D)	82.83(15)
Sm(1)–O(4)	2.331(3)	O(1F)–Cu(1)–O(3)	89.33(14)	O(2)–Sm(1)–O(4E)	152.06(13)
		O(1A)–Sm(1)–O(2A)	68.59(12)	O(2)–Sm(1)–O(1B)	124.82(12)
		O(1A)–Sm(1)–O(4C)	81.96(13)	O(1B)–Sm(1)–O(4E)	84.96(13)
		O(2A)–Sm(1)–O(4C)	79.56(12)	O(1)–Sm(1)–O(4D)	81.96(13)

Table 3
Hydrogen bond distances (Å) and angles (°) for complexes **1**

Complex	Hydrogen bond	Distance	Angle	Symmetry code
1	N1–H1···O2	2.936	151.61	$x-y$, $x-1$, $-z$
	O5–H5a···O3	3.150	162.35	$-x+2$, $-y-1$, $-z$
	O5–H5a···O4	3.238	149.28	x, $x-y-2$, $z-1/2$
	O6–H6b···O5	3.213	129.97	

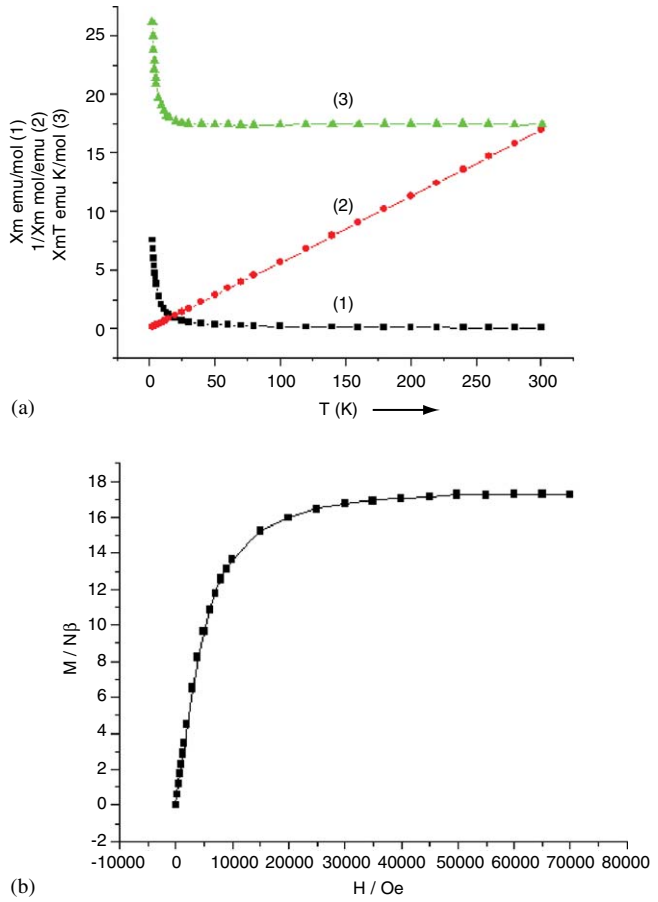

Fig. 4. For complex **2**: (a) Plot of the temperature dependence of $\chi_m T$ (▲), χ_m (■) and $1/\chi_m$ (●) for $[\{Gd_2Cu_3(Idad)_6\}\cdot 8H_2O]_n$ measured at 1 T field; and (b) magnetization M vs. magnetic field H curves for compound **2** at 2 K.

magnetic chemistry property has not been investigated up to now. Allowing for the special property of Gd(III) ion, the Gd(III)–Cu(II) compound with similar structure (its compositions, $[\{Gd_2Cu_3(Idad)_6\}\cdot 8H_2O]_n$, was confirmed by EA and XRD spectra) was selected for the study of its magnetic behavior. The variable-temperature magnetic susceptibility of these compounds in the temperature range 2–300 K at an applied field of 1 T was measured; the $\chi_{m,1}/\chi_m$ and $\chi_m T$ vs. T plots of magnetic susceptibility data for the compound is shown in Fig. 4(a).

For the compound $[\{Gd_2Cu_3(Idad)_6\}\cdot 8H_2O]_n$, the values of $\chi_m T$ are basically constant from 300 to 15 K (average value 17.3 emuK/mol), and then this is a steady rise in $\chi_m T$ below 15 K. The experimental value of $\chi_m T$ is was 17.25 emuK/mol at room temperature, which is slightly higher than the theoretical value 16.87 emuK/mol (two Gd(III) and three Cu(II)). The observed susceptibility data are obey the Curie–Weiss law ($\chi_m = C/(T-\Theta)$), with Weiss constant $\Theta = 0.5245$ K and $C = 17.3628$ emu K/mol, indicating a weak ferromagnetic behavior.

The field dependence of the magnetization measured at 2.0 K is showed in Fig. 4(b) in the form of a M vs. H plot, where M and H are magnetization and applied magnetic field, respectively. It is expected from the above magnetic susceptibility data that only the ground state ($S = 17/2$) is significantly populated at 2 K. As expected, the magnetization behavior at 2 K follows the Brillouin function of $S = 17/2$ very well, indicating the operation of a possible ferromagnetic interaction between Cu^{II} and Gd^{III} to give the ground state of $S = 17/2$, which is almost completely populated at 2 K. Thus, a ferromagnetic spin-spin interaction between Cu^{II} and Gd^{III} appears to operate in the present complex, as observed in the previously prepared CuGd, Cu_4Gd_2 and Cu_3Dy_2 complexes [15]. Detailed studies on magnetic properties and the other polymer lanthanide–transition metal complexes are underway and will be reported later in a full paper.

3.4. Strategies of assembly

Ligand design or selection is often a useful way of manipulating the overall structural order and the properties of compounds. The organic building blocks for constructing coordination three-dimensional networks of zeolite-type are most often rigid bridging ligands, either liner or disk-shaped trigonal-planar; flexible organic ligands are used less often. However, because of the high coordination numbers of lanthanide ions and the variable coordination numbers (generally, 4–6) of copper ions, the ligand with appropriate flexibility will contribute to syntheses of multidimensional channel systems and novel structures with micropores. For the previous reported compounds $[\{Ln_4Cu_2(pydc)_8(H_2O)_8\}\cdot 18H_2O]_n$ (Ln = La (1); Pr (2)) (H_2pydc = pyridine-2,6-dicaboxylic acid), two carboxyl groups of the rigid ligand $pydc^{2-}$ take (3) and (4) two coordination forms to coordinate with lanthanum and copper ions respectively, thus a one dimensional chain was obtained, and finally O–H···O hydrogen bonds and $\pi\cdots\pi$ stacking interactions between 1D infinite chains generate an open, three-dimensional network. For present compound $[\{Sm_2Cu_3(Idad)_6\}\cdot 8H_2O]_n$, the flexible ligand $Idad^{2-}$are

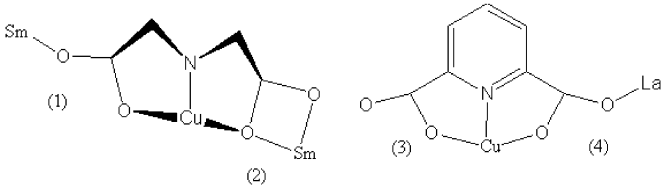

used as reagent (in reaction with CuO and Sm_2O_3) and its two arms present a butterfly like pattern; accordingly two carboxyl groups adopt (1) and (2) two coordination modes to coordinate with samarium and copper ions respectively, and the resulting product has an open framework with an intersecting 3D channel system. This result may provide a new way to adjust the flexibility of organic ligands and to control the coordination mode of organic ligands in the lanthanide–transition metal reaction systems, which are useful for the designing of model complexes with nanopores for magnetic materials.

Acknowledgments

We are grateful to the National Natural Science Foundation of P. R. China, and the N.S.F. of Guangdong Province for financial support.

Appendix A. Supplementary Data

Supplementary data associated with this article can be found in the online version at doi:10.1016/j.jssc.2005.09.033.

References

[1] (a) M.J. Zaworotko, Nature 386 (1997) 220;
(b) T.E. Mallouk, Nature 387 (1997) 350;
(c) H. Li, M. Eddaoudi, M. O'Keeffe, O.M. Yaghi, Nature 402 (1999) 276;
(d) J.S. Seo, D.G. Wheng, S.I. Jun, J.H. Oh, Y.J. Jeon, K.K. Kim, Nature 404 (2000) 982.

[2] (a) C. Janiak, Angew. Chem. Int. Ed. Engl. 36 (1997) 1431;
(b) S.S.-Y. Chui, S.M.-F. Lo, J.P.H. Charmant, A.G. Orpen, I.D. Williams, Science 283 (1999) 1148.

[3] Y.-C. Liang, M.-C. Hong, W.-P. Su, R. Cao, W.-J. Zhang, Inorg. Chem. 40 (2001) 4574.

[4] (a) D.M.J. Doble, C.H. Benison, A.J. Blake, D. Fenske, M.S. Jackson, R.D. Kay, W.-S. Li, M. Schröder, Angew. Chem. Int. Ed. Engl. 38 (1999) 1915;
(b) Y.-C. Liang, R. Cao, W.-P. Su, M.-C. Hong, W.-J. Zhang, Angew. Chem. Int. Ed. Engl. 39 (1999) 3304.

[5] (a) J.J. Lu, A. Mondal, B. Moulton, M.J. Zaworotko, Agew. Chem. Int. Ed. Engl. 40 (2001) 2113;
(b) M. Eddaoudi, D.B. Moler, H.L. Li, B.L. Chen, T.M. Reineke, M. O'Keeffe, O.M. Yaghi, Acc. Chem. Res. 34 (2001) 133;
(c) R. Kitaura, K. Noro, S.-L. Fujimoto, M. Kondo, S. Kitagawa, Agew. Chem. Int. Ed. Engl. 41 (2002) 113;
(d) A. Escuer, R. Vicente, F.A. Mautner, M.A.S. Goher, M.A.M. Abu-Youssef, Chem. Commun. 64 (2002) 64;
(e) D.T. Vodak, M.E. Braun, J. Kim, M. Eddaoudi, O.M. Yaghi, Chem. Commun. (2001) 2534.

[6] (a) R.E. Melendez, C.V.K. Sharma, M.J. Zaworotko, C. Bauer, R.D. Rogers, Angew. Chem. Int. Ed. Engl. 35 (1996) 2213;
(b) Y.-B. Dong, M.D. Smith, H.-C. Zur Loye, Agew. Chem. Int. Ed. Engl. 39 (2000) 4271;
(c) R.J. Doedens, E. Yohannes, M.I. Khan, Chem. Commun. (2002) 62;
(d) D.M. Ciurtin, M.D. Smith, H.-C. Zur Loye, Chem. Commun. (2002) 74.

[7] (a) Z. Shi, S.-H. Feng, S. Gao, L.-R. Zhang, G.Y. Yang, J. Hua, Agew. Chem. Int. Ed. Engl. 39 (2000) 2325;
(b) Y.-P. Ren, L.-S. Long, B.-W. Mao, Y.-Z. Yuan, R.-B. Huang, L.-S. Zheng, Agew. Chem. Int. Ed. Engl. 42 (2003) 532.

[8] (a) C.-Y. Su, B.-S. Kang, H.-Q. Liu, Q.-G. Yang, Thomas C.W. Mak, Chem. Commun. (1998) 1551;
(b) C.-Y. Su, B.-S. Kang, Q.-G. Yang, Thomas C.W. Mak, J. Chem. Soc. Dalton Trans. (2000) 1858;
(c) C.-Y. Su, B. -S. Kang, C.-X. Du, Q.-G. Yang, Thomas C.W. Mak, Inorg. Chem. 39 (2000) 4843.

[9] Y.-P. Cai, C.-Y. Su, C.-L. Chen, Y.-M. Li, B.-S. Kang, A.S.C. Chan, W. Kaim, Inorg. Chem. 42 (2003) 163.

[10] C.-Y. Su, X.-P. Yang, B.-S. Kang, Thomas C.W. Mak, Agew. Chem. Int. Ed. Engl. 40 (2001) 1775.

[11] G.M. Sheldrick, SADABS. Program for Scaling and Correction of Area Detector Data, University of Göttingen, Göttingen, Germany, 1996.

[12] SHELXTL, Ver. 5.10, Bruker Analytical X-ray Systems, Madision, WI, USA, 1998.

[13] O.M. Yaghi, C.E. Davis, G.G. Li, H.L. Li, J. Am. Chem. Soc. 119 (1997) 2861.

[14] J.-G. Mao, L. Song, X.-Y. Huang, J.-S. Huang, Polyhedron 16 (1997) 963.

[15] (a) M. Manseki, Y. Kitakami, M. Sakamoto, H. Sakiyama, Y. Nishida, A. Matsumoto, Y. Sadaoka, Y. Nishida, M. Sakai, Y. Fukuda, M. Ohba, H. Okawa, J. Coord. Chem. 48 (1999) 1;
(b) O. Guillou, P. Bergerat, O. Kahn, E. Bakalbassis, K. Boubekeur, P. Batail, M. Guillot, Inorg. Chem. 31 (1991) 110;
(c) O. Guillou, O. Kahn, R.L. Oushoorn, K. Boubekeur, P. Batail, Inorg. Chim. Acta 198–200 (1992) 119–131.